

# OBTAINING SUB-PICOSECOND X-RAY PULSES IN THE ADVANCED PHOTON SOURCE USING LASER SLICING\*

A. Zholents<sup>†</sup>, M. Borland, ANL, Argonne, IL 60439, USA

## Abstract

The laser slicing technique [1] has been successfully applied at several low- to medium-energy storage ring light sources to create sub-picosecond pulses of x-rays. Application to high-energy storage rings has been considered problematic because of the required average laser power. However, because of on-going advances in laser technology, this technique is now within reach at light sources like the Advanced Photon Source (APS), which operates at 7 GeV. In this paper, we analyze the potential performance of laser slicing at APS, and compare it to alternatives such as deflecting cavities.

## INTRODUCTION

APS is pursuing short x-ray pulse production using the deflecting cavity scheme [2], as described in [3], promising 1-ps FWHM pulses with 1% of normal x-ray flux [4]. Another method of obtaining short x-ray pulses from storage rings is using “laser-slicing.” This technique [5], which involves using a laser to increase the energy spread of a short slice of the bunch, was first demonstrated at ALS [1], producing ~100-fs x-ray pulses with few-kHz repetition rates. In addition, BESSY-II [6] and SLS [7] also routinely use slicing for time-resolved pump-probe experiments. SOLEIL plans to add slicing to their machine [8] and is considering an upgrade option [9] that employs echo-enabled harmonic generation [10].

In this concept, a short laser pulse interacts with a section of the electron beam in a wiggler. In order for this interaction to modulate the energy of the electrons, the resonance condition  $\lambda_W = \frac{2\lambda_L\gamma^2}{1+K^2/2}$  must be satisfied, with  $\lambda_W$  the wiggler wavelength,  $\lambda_L$  the laser wavelength,  $\gamma$  the electron beams’ relativistic factor ( $1.37 \times 10^4$  for APS), and  $K = eB_W\lambda_W/(2\pi m_e c)$  the wiggler strength parameter for peak wiggler field  $B_W$ . A readily apparent difficulty is that  $\lambda_W \propto \gamma^2$ . Indeed, all of the light sources listed above operate between 2 GeV and 3 GeV, allowing use of a relatively compact wiggler magnet that easily fits in a straight section while still having a large number of wiggler periods to facilitate the laser-electron beam interaction.

In a 7 GeV facility like the APS, one would need a much longer wavelength device. This can be mitigated somewhat by making  $K\lambda_W[m] \gg 1$ , giving  $\lambda_W \approx 0.077 \sqrt{\lambda_L\gamma^2/B_W^2}$ , however, we still have  $\lambda_W \sim \gamma^{2/3}$ . In addition, very large  $B_W$  in a high-energy ring may cause

excessive power loads and emittance degradation. Hence, a wiggler in the higher energy machine with the same number of periods as the wiggler in the lower energy machine (which is prudent for a more effective interaction of the electrons with the laser), will occupy significantly more real estate. In the following numerical examples we use a 4.7-m-long wiggler with  $B_W = 1.5T$ . This wiggler would slightly increase the energy spread and effective emittance, due to dispersion in the straight sections. A likely candidate for a short-pulse laser a Ti:sapphire system operating at a harmonic  $h$  of its fundamental wavelength  $\lambda_L = 0.8\mu\text{m}$ . If  $B_W = 1.5\text{ T}$  and  $h = 1$ , then  $\lambda_W = 31\text{ cm}$  and  $K = 43$ . At most 15 periods of such a device can be accommodated in a standard APS straight section. The device will produce a manageable 70 kW of radiation power at 200 mA.

## CHOICE OF LASER HARMONIC

Electrons that co-propagate with the laser pulse through a wiggler are accelerated or decelerated depending on the phase  $\phi$  of the laser field seen by each electron at the entrance of the wiggler. The figure of merit for slicing is the ratio of the amplitude of this energy modulation  $\Delta E$  to the rms electron beam energy spread  $\sigma_E$ . It can be approximated with a good accuracy using [5, 11]

$$\frac{\Delta E}{\sigma_E} = 2 \left( \frac{A_L A_W}{\sigma_E^2} \frac{M_W/\xi}{M_L} \eta_{emit} \right)^{\frac{1}{2}}, M_W/\xi \leq M_L, \quad (1)$$

with  $A_L$  the laser pulse energy,  $M_W$  the number of wiggler periods,  $M_L$  the number of optical cycles in the FWHM laser pulse length, and  $A_W \approx 2.5\alpha\hbar\omega_L$  the energy spontaneously emitted in the fundamental mode of wiggler radiation by a single electron passing through the wiggler with  $K \gg 1$  [12, 11]. ( $\alpha$  is the fine structure constant,  $\hbar$  is Planck’s constant, and  $\omega_L = 2\pi c/\lambda_L$ .) Since each electron slips through  $M_W$  optical cycles in traversing the wiggler, increasing the laser pulse length beyond  $M_W/\xi$  cycles does not increase the energy exchange, where the factor  $\xi \approx 1.4$  results from matching the spectrum of a laser pulse (assumed to be Gaussian) to the sinc-function spontaneous emission spectrum from the wiggler [12].

The non-zero size and divergence of the electron beam contributes to some loss in the amplitude of the energy modulation integrated over the transverse distribution of electrons. This is accounted for in Eq. 1 by the coefficient  $\eta_{emit} \approx w_0^2/(w_0^2 + 2\sigma_x^2)$  [1], with  $\sigma_x$  the rms electron beam size,  $w_0 = \sqrt{Z_R\lambda_L/\pi}$  the laser waist size, and  $Z_R$  the Rayleigh length. Taking  $Z_R \geq L_W/4$  maximizes  $\Delta E$  [13], implying  $\lambda_L \gg 8\pi\sigma_x^2/L_W$  in order to obtain  $\eta_{emit} \rightarrow 1$ . According to Eq. 1, this also helps to maximize

\*Work supported by the U.S. Department of Energy, Office of Science, Office of Basic Energy Sciences, under Contract No. DE-AC02-06CH11357.

<sup>†</sup>azholents@aps.anl.gov

$\Delta E$ . For example, in the case of APS, using a lattice with reduced beam size of  $\sigma_x = 200\mu\text{m}$  in the wiggler straight and  $L_W = 4.7$  m, we obtain  $\lambda_L \gg 0.2\mu\text{m}$ . Assuming use of a Ti:Sapphire laser, one can thus safely consider using its second harmonic (wavelength of  $0.4\mu\text{m}$ ), while using its third harmonic will cause a drop in  $\Delta E$ .

Let us now explore which harmonic is better, assuming fixed wiggler length. We note that  $A_W \sim \lambda_L^{-1}$  and  $M_L \sim \lambda_L^{-1}$ . Also, since for a given  $B_W$  one has  $\lambda_W \sim \lambda_L^{1/3}$ , we have  $M_W \sim \lambda_L^{-1/3}$ . Thus, we have in Eq. 1  $A_W M_W / M_L \sim \lambda_L^{-1/3}$ . Therefore, to obtain the same  $\Delta E / \sigma_E$  using the second harmonic as using the first, one needs less laser pulse energy by the factor  $(0.4/0.8)^{-1/3} = 2^{1/3}$ . However, assuming a 50% first-to-second-harmonic conversion efficiency, we would need a Ti:Sapphire laser with a factor  $2^{2/3}$  more laser power if we operate at the second harmonic. Thus, using the first harmonic is a more efficient way to obtain large  $\Delta E / \sigma_E$ .

To verify this result, we calculated the Ti:Sapphire laser pulse energy required to obtain a given  $\Delta E / \sigma_E$  for two working harmonics (first and second) and FWHM pulse duration  $\tau_L = 50$  fs. Initially, we assumed  $\eta_{emit} = 1$ , obtaining the dotted curves shown in Fig. 1. These confirm the expected  $2^{2/3}$  ratio. Including the effect of electron beam size reduces the energy modulation more strongly at shorter laser wavelength, as apparent from the solid curves in Fig. 1.

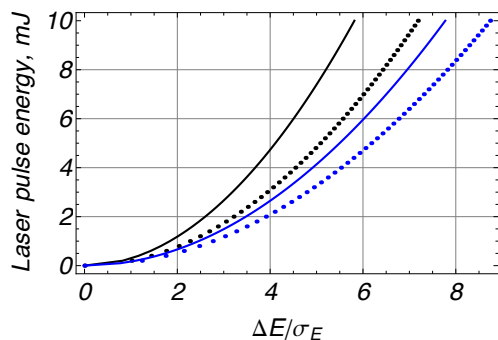


Figure 1: Laser pulse energy at Ti:Sapphire fundamental wavelength as a function of the relative amplitude of the energy modulation. The black (blue) curves are for first (second) harmonic operation. The solid curves include electron beam size effects, while the dotted curves assume  $\sigma_x = 0$ . 50% second-harmonic conversion efficiency is assumed.

Next, we simulated the laser/electron beam interaction using eLégant [14], in order to numerically explore the optimum waist size. Fig. 2 shows results for operation at the first and second harmonics, assuming 50% conversion efficiency for the second harmonic. In order to bring the laser beam into the straight section for interaction with the wiggler, we must put optical elements upstream of the nearest dipole, at a minimum distance of  $\sim 14$  m from the waist. The laser beam size ( $2\sigma$ ) at that distance will be  $\approx 10w_0$ , or 6 mm for the  $0.8\mu\text{m}$  case. The APS vacuum cham-

ber has an ante-chamber with a narrow neck that will not cleanly pass a gaussian beam this size, so a modified chamber would be required. This highlights another relative difficulty for high-energy rings, namely, the greater length of the magnets and the smaller angle of the dipoles.

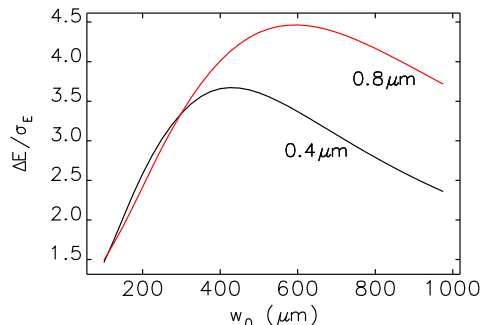


Figure 2: Results of eLégant simulation of the interaction of the electron bunch for two Ti:Sapphire harmonics assuming constant fundamental laser pulse energy of 4 mJ and 50% conversion efficiency for the second harmonic.

## OTHER CONSIDERATIONS

As in [6], we consider selection of the femtosecond x-ray pulses using angular separation. Ideally, the lattice should be optimized for this application, however, for now we use the standard APS lattice. We model a single pass dispersion function  $D$  beginning from the wiggler straight section and obtain two sectors downstream  $D' = -8.2 \times 10^{-3}$ , where  $D = dD/ds$ . At this location the time-off-flight dispersion due to the electron beam energy spread is  $\tau_D \approx 115$  fs FWHM. Thus, the anticipated FWHM x-ray pulse duration is  $\tau_{x\text{-ray}} = \sqrt{\tau_L^2 + \tau_D^2} \approx 125$  fs. (A 75 fs FWHM x-ray pulse can be obtained if the undulator is located one sector downstream of the wiggler. However, this requires further investigation as it will require a non-standard lattice.) If we further assume  $\Delta E = 5\sigma_E$ , we find  $\Delta x'_{x\text{-ray}} = D' \Delta E / E \approx 40\mu\text{rad}$  as the extremal angle of the electron trajectory in the undulator. The goal is to have this angle larger by at least a factor of five than angular divergence of the photon beam emitted by the bulk of the electron beam (approximately  $12\mu\text{rad}$  for  $1\text{\AA}$  radiation). This allows clear separation of a short x-ray pulse coming from the energy modulated electrons from the radiation of the rest of electrons. Evidently, we need to increase  $D'$  by  $\sim 30\%$  to reach our goal, which we believe can be done with a special lattice. According to Figs. 1 and 2, reaching this goal requires laser pulse energy of  $\sim 4$  mJ.

A complementary result of the slicing technique is creation of a small dip in the electron distribution along the electron bunch, whose depth and width evolves as the electron bunch propagates around the ring. This density modulation causes a coherent synchrotron radiation with a spectrum extended up to  $\sim 10$  THz (if the THz pulse is taken in the sector nearest to the wiggler). We assume that this

radiation will be mostly obstructed by the vacuum chamber and, thus, only a small fraction can be extracted. Still, it should be sufficient for a diagnostic of the laser interaction, whose impact can be followed even after several turns of the electron bunch around the ring due to the high signal to noise level of coherent radiation [6].

The maximum repetition rate may be limited by the laser power, the tolerable increase in the electron beam energy spread, and signal-to-noise considerations. To mitigate the latter two issues, we consider a multi-bunch beam, where each bunch is targeted in turn. To estimate the energy spread increase, one first looks at the energy change of an electron during a single turn when the laser hits the bunch. For the  $i^{\text{th}}$  electron

$$\Delta E_i = (QE)_i + p\sigma_E \sin \omega_L t_i \exp \left\{ -\frac{t_i^2}{2\sigma_L^2} \right\}, \quad (2)$$

where  $(QE)_i$  is a random deviate representing quantum excitation,  $p = \Delta E/\sigma_E$ , and  $\sigma_L$  is the rms laser pulse duration. Averaging this over the electron bunch gives

$$\langle \Delta E^2 \rangle = \mathcal{N}\langle u^2 \rangle T_0 + \frac{p^2 \sigma_E^2 \sigma_L}{4\sqrt{2}\sigma_B}, \quad (3)$$

where  $\mathcal{N}\langle u^2 \rangle$  is the familiar quantum excitation term [15],  $T_0$  is the revolution time, and  $\sigma_B$  is the rms electron bunch duration. The effective excitation rate is

$$\frac{d}{dt} \langle \Delta E^2 \rangle = \mathcal{N}\langle u^2 \rangle + \frac{p^2 \sigma_E^2 \sigma_L f_L}{4\sqrt{2}\sigma_B n_b}, \quad (4)$$

where  $f_L$  is the laser repetition rate and  $n_b$  is the number of bunches. The equation for the equilibrium energy spread is [15]

$$\sigma_E^2 = \frac{1}{4} \tau_E \frac{d}{dt} \langle \Delta E^2 \rangle = \sigma_{E0}^2 \left( 1 + \frac{p^2 \sigma_L f_L \tau_E}{16\sqrt{2}\sigma_B n_b} \right). \quad (5)$$

If  $\sigma_E$  is allowed to grow by 10%, then we have

$$f_L \leq \frac{16\sqrt{2}\sigma_B n_b}{5p^2 \sigma_L \tau_E}. \quad (6)$$

For  $p = 5$ ,  $\sigma_B = 50$  ps,  $n_b = 24$ ,  $\sigma_L = 50/2.35$  fs, and  $\tau_E = 4.8$  ms, one has  $f_L \leq 2$  MHz. This is much larger than the repetition rate of available lasers and hence not a limiting factor. Indeed, the signal-to-noise requirement will limit the rate to  $\sim n_b/\tau_E \approx 5$  kHz.

## FLUX ESTIMATE

We estimated the x-ray flux assuming 24, 15-nC electron bunches (100 mA total) with  $\sim 150$  ns bunch spacing and a FWHM electron bunch length of  $\sim 100$  ps. 30-W average power Ti:Sapphire lasers are commercially available, supporting 6.5 kHz operation for our required 4 mJ pulse energy.

For an APS-standard 2.4-m-long, 3.3-cm-period undulator producing 1Å radiation, we have  $3 \times 10^7$  photons/pulse/0.1%BW. Multiplying by the ratio of pulse

lengths  $50 \text{ fs}/100 \text{ ps} \approx 5 \times 10^{-4}$  and recognizing that only  $\sim 5\%$  of the photons will receive the full energy modulation implies  $\sim 750$  photons/pulse/0.1%BW or  $5 \times 10^6$  photons/s/0.1%BW at 6.5 kHz.

In comparison, for the crab cavity scheme we have  $3 \times 10^5$  photons/pulse/0.1%BW, about 400 times greater than for laser slicing. The repetition rate is 6.5 MHz, giving an average flux that is  $4 \times 10^5$  higher than laser slicing. Further, use of asymmetric cut crystals to compress the chirped x-ray pulse [2] can potentially increase this by another order of magnitude [16]. Hence, the crab cavity scheme has a significant flux advantage, provided the  $\sim 1$  ps FWHM x-ray pulses are acceptable.

## CONCLUSION

We have demonstrated the feasibility of the slicing technique at the APS, in spite of the high beam energy. We believe that x-ray pulses with  $\sim 125$  fs FWHM pulse duration, fluxes of  $\sim 750$  photons/pulse/0.1%BW or  $\sim 5 \times 10^6$  photons/second/0.1%BW can be produced. It would require a laser producing 50 fs pulses with 4 mJ energy per pulse at a 6.5 kHz repetition rate. An x-ray pulse with a 75 fs FWHM pulse duration can be obtained if the undulator is located one sector downstream of the wiggler. We also note that the implementation of the slicing technique at the APS would require a modified vacuum chamber to ensure efficient transport of the laser through the bending magnet to the wiggler straight section.

Laser slicing, like the crab cavity scheme, has the advantage that it is in principle largely invisible to other users. Both can be used at our full, normal operating current of 100 mA in 24 bunches as well as at higher current in the future. Of the two, the crab cavity scheme promises five orders of magnitude higher flux, but ten-fold longer x-ray pulses. We consider the crab cavity scheme the best match to the requirements of APS users.

## REFERENCES

- [1] R. W. Schoenlien et al., Science, March 24, 2000: 2237.
- [2] A. A. Zholents et al., NIMA 425 (1999) 385.
- [3] K. Harkay et al., Proc. 2005 PAC, p. 668 (2005).
- [4] M. Borland et al., Proc. 2005 PAC, p. 3886 (2005).
- [5] A. A. Zholents et al., Phys. Rev. Lett. 76 (1996) 912.
- [6] S. Khan et al., PRL 97 (2006) 074801.
- [7] V. Schlott et al., Proc. EPAC2004, p. 1229 (2004).
- [8] A. Nadji et al., Proc. EPAC2004, p. 2332 (2004).
- [9] C. Evain et al., Advanced Photon Source LS-322 (2010).
- [10] G. Stupakov, PRL 102 (2009) 074801.
- [11] A. Zholents et al., Proc. FEL06, p. 725 (2006).
- [12] D. E. Alferov et al., Particle Accel. 9 (1979) 223.
- [13] A. Amir et al., NIMA 250 (1986) 404.
- [14] M. Borland, Advanced Photon Source LS-287 (2000).
- [15] M. Sands, SLAC Report SLAC-121 (1979).
- [16] S. Shastri, private communication.